DR. GIUSEPPE OTTRIA (Orcid ID : 0000-0002-0797-5500)

Article type : Paper

Received date: 07-Jun-2017
Revised version received date: 30-Aug-2017
Accepted date: 13-Sep-2017

Evolution of an early Eocene pull-apart basin in the Central Pontides (Northern Turkey): new insights into the origin of the North Anatolian Shear Zone

Giuseppe Ottria[1*], Luca Pandolfi[2,1], Rita Catanzariti[1], Simone Da Prato[1], Alessandro Ellero[1], Chiara Frassi[2], Mehmet Cemal Göncüoğlu[3], Michele Marroni[2,1], Leonardo Ruffini[2], Kaan Sayit[3]

[1]Istituto di Geoscienze e Georisorse - CNR, Via G. Moruzzi 1, 56124, Pisa, Italy, email: ottria@igg.cnr.it, catanzariti@igg.cnr.it, daprato@igg.cnr.it, ellero@igg.cnr.it

[2]Dipartimento di Scienze della Terra, Università di Pisa, via S. Maria 53, 56126, Pisa, Italy, email: pandolfi@dst.unipi.it, chiarafrassi@gmail.com, marroni@dst.unipi.it,

[3]Department of Geological Engineering, Middle East Technical University, 06800 Ankara, Turkey, email: mcgoncu@metu.edu.tr, ksayit@metu.edu.tr

*Corresponding author: tel: +39 050 2215747; email: ottria@igg.cnr.it

This article has been accepted for publication and undergone full peer review but has not been through the copyediting, typesetting, pagination and proofreading process, which may lead to differences between this version and the Version of Record. Please cite this article as doi: 10.1111/ter.12299

ABSTRACT

Although the North Anatolian Shear Zone is one of the main lithospheric-scale strike-slip deformation zones in the world, playing a prominent role in the complex geodynamic interaction between the Eurasian, Anatolian and Arabian plates, the onset time of its activity remains highly controversial. Here, we tackle this issue by utilizing nannofossil biostratigraphy on deposits from the Taşcilar basin, a pull-apart basin that we have identified inside the North Anatolian Shear Zone overprinting the Intra-Pontide suture zone. The syn-tectonic sedimentary succession of the Taşcilar basin developed completely during the early Eocene (Ypresian; CNE4–CNE5 Zones). The strike-slip faulting related to the initial onset of the North Anatolian Shear Zone can likely be constrained within the Ypresian, suggesting that the westward escape of the Anatolian plate along the North Anatolian Shear Zone started in the early Eocene.

1. INTRODUCTION

The North Anatolian Shear Zone (NASZ; Şengör et al., 2005; Ellero et al., 2015a), representing the collision zone between the Anatolian and Eurasian plates, provides a global case study of a continental plate boundary. The NASZ is developed as a broad, up to 100 km wide, deformation zone across all of northern Turkey, extending for more than 1400 km in an approximately E–W direction (Figure 1). Along its western and central branches, the NASZ overprints the Intra-Pontide suture zone, an ophiolitic suture originating from the continental collision between two terranes of Eurasian affinity (i.e. the Istanbul-Zonguldak and Sakarya terranes) originally separated by a branch of the Neotethys (i.e. Intra-Pontide ocean) (Okay & Tüysüz, 1999).

The NASZ is characterized by systems of strike-slip faults and associated structures showing an overall right-lateral displacement. Within the NASZ, several pull-apart basins have developed

(Barka et al., 2000; Şengör et al., 2005). Based on the ages of the fault-related basin deposits, the onset of NASZ activity is commonly constrained to the late Miocene (Şengör et al., 2005 and references therein). However, the timing of NASZ onset is still controversial, and different ages have been proposed (Barka, 1992; Armijo et al., 1999; Koçyiğit et al., 2001; Hubert-Ferrari et al., 2002, 2009; Zattin et al., 2005, 2010; Uysal et al., 2006; Boles et al., 2015; Türkoğlu et al., 2016).

The multidisciplinary study (structural geology, sedimentological and micropalaeontological analyses and volcanic geochemistry) that we carried out within the bending area of the NASZ identified an early Eocene pull-apart basin, namely the Taşcilar basin, suggesting the early Eocene as the onset age of the NASZ. This timing constraint for the initiation of NASZ activity contributes to the discussion of the post-collisional geodynamic evolution of the Anatolian plate.

2. TECTONIC SETTING OF THE TAŞCILAR BASIN

The Taşcilar basin is an approximately 5 km long and 2 km wide basin located within the central bend of the NASZ (Figure 2; Appendix S1). The Taşcilar basin unconformably developed inside two tectonic units belonging to the imbricate stack of the Intra-Pontide suture zone (Göncüoğlu et al., 2008, 2012; Okay et al., 2013; Frassi et al., 2016; Sayit et al., 2016): the Upper Cretaceous ophiolite-bearing Arkot Dağ Mélange (Göncüoğlu et al., 2014) and the Domuz Dağ metamorphic Unit (Okay et al., 2006). The basin shows a roughly trapezoidal shape and is bounded by a complex network of high-angle faults, where the master faults, corresponding to the northern and southern margins of the basin, are parallel to the NASZ system (Figure 2). The complex fault array, which includes cross-basin faults that link the master fault offset, was responsible for localized intrabasinal subsidence, separating different depocentres inside the basin. The tectonic-controlled architecture is also responsible for the sudden lateral facies changes that can be observed both on geological maps and in cross-section (Figure 2; Appendix S1). The basement-involved faulting was accompanied by subalkaline basaltic volcanism (Figure 2; see Section 4).

The brittle structural analysis performed in the Taşcilar basin area highlighted that faults are predominantly high-angle strike-slip faults trending along three main directions (Figure 3), locally displaying cataclastic zones (Appendix S2). Clear cross-cutting relationships between different faults, or fault planes bearing multiple generations of slickenlines, were not detected during the fieldwork.

The palaeostress reconstructions indicate two different stress tensors characterized by sub-vertical σ_2 intermediate stress axes. The first one displays a sub-horizontal σ_1 axis directed NE–SW, which is consistent with ENE–WSW-trending sinistral strike-slip faulting and roughly N–S dextral strike-slip faulting (Figure 3d). The second stress tensor has a WNW–ESE-directed σ_1 axis and matches NE–SW-trending dextral strike-slip faults with NW–SE-directed sinistral strike-slip faults (Figure 3e). This latter stress tensor is consistent with palaeostress directions elaborated for adjacent NASZ sectors (Ellero et al., 2015a), where the strain partitioning is characterized by transpression. This feature is also evidenced in the Taşcilar basin, by reverse faults that segment the stratigraphic succession (Figure 2b).

3. STRATIGRAPHIC EVOLUTION OF THE TAŞCILAR BASIN

The stratigraphic succession of the Taşcilar basin includes three formations, which are, from the bottom to the top, the Delibey, the Taşcilar and the Hatip Formations (Figures 2, 4 and 5). The Delibey Formation shows facies associations characteristic of hyperconcentrated flood flow developed in a mass-flow-dominated alluvial fan (cf. Nemec & Steel, 1984). This formation grades to the overlying Taşcilar Formation, interpreted as shallow-marine deltaic deposits. The Taşcilar Formation shows a transition from a lower part characterized by high-density small-volume flows developed in a steep depositional environment such as a delta slope and/or delta front (cf. Sohn et al., 1997), to an upper part characterized by deposits from the frontal margin of a relatively deep fluvial-influenced mouth bar (cf. Sohn & Son, 2004). Subalkaline basalts are interbedded as syn-sedimentary pillow lavas in poorly lithified sediments in the uppermost part of the Taşcilar Formation (Figure 6a). The Hatip Formation, which is separated from the Taşcilar Formation by an angular unconformity (Figure 4f), is interpreted as a coarse shallow-marine inner-deltaic system strongly influenced by fluvial floods. Overall, the clasts of the Taşcilar basin succession are dominated by lithologies from the units of the underlying Intra-Pontide suture zone basement. The Taşcilar and Hatip Formations were sampled in order to identify the depositional age and environments of the Taşcilar basin (Appendix S3).

3.1. Nannofossil Biostratigraphy

We collected 41 marly mudstone samples, of which 39 samples contained well- to poorly preserved calcareous nannofossils varying in abundance from abundant to few (Figure 5; Appendix S4). The lower 50 metres of the sampled Taşcilar section contain 12 samples with well-preserved calcareous nannofossil specimens that include *Dictyococcites* sp., *Reticulofenestra dictyoda*, *Coccolithus crassus*, *Tribrachiatus orthostylus*, *Girgisia gammation*, *Toweius* spp., *Discoaster lodoensis*, *Discoaster kuepperi* and *Discoaster barbadiensis*. This assemblage can be attributed to the upper part of the early Eocene CNE4 Zone of Agnini et al. (2014), characterized by the co-occurrence of *C. crassus* and Noelaerhabdaceae members (*R. dictyoda* and *Dictyococcites*), *T. orthostylus* and *Toweius* spp., and roughly corresponding to the upper part of C23n and the lowermost part of C22r (Appendix S3), with an age estimated between 50.93 Ma (age of the lowest occurrence of *C. crassus*) and 50.66 Ma (age of the highest occurrence of *T. orthostylus*). Twenty samples coming from the remaining 250 m of the Taşcilar Formation contain Noelaerhabdaceae members, *Toweius* spp. and *C. crassus* and can be attributed to the early Eocene CNE5 Zone, constrained between the highest occurrence of common and continuous *T. orthostylus* and the lowest occurrence of *Discoaster sublodoensis*. In the upper part of the Taşcilar Formation, seven samples from a 6 metre thick level are characterized by assemblages containing *T. orthostylus* and *Toweius* spp. without Noelaerhabdaceae members, which point to the lower part of the CNE4 Zone, suggesting that intrabasinal landslides triggered by the tectonic activity of the basin margins reworked part of the older succession. Only one sample from the Hatip Formation yielded calcareous nannofossils that allowed biostratigraphic characterization. The occurrence of high proportions of *R. dictyoda*, *Dictyococcites* sp. and *Cyclicargolithus floridanus* (Noelaerhabdaceae), which bloom in the middle part of the CNE5 Zone (Agnini et al., 2014), suggests a biostratigraphic position corresponding to the upper part of the CNE5 Zone.

3.2. Ostracods and Benthic Foraminifera

Eleven samples were collected for analysis of ostracods and benthic foraminifera (Figure 5; Appendix S5). The sampled section is characterized by ostracods that testify to a bathymetric decrease from an upper bathyal (with *Dutoitella eocenica*, *Legitimocythere presequenta*, *Trachyleberidea pisinensis*, *Bairdia ilaroensis* and *Cytherella* gr. *serratula*) to an outer neritic environment (with *B. ilaroensis* and *C.* gr. *serratula* and without *D. eocenica*, *L. presequenta* and *T. pisinensis*) (Dall'Antonia et al., 2003). Benthic foraminifera recognized in the Taşcilar

Formation testify to a wider bathymetric range from outer neritic to upper bathyal. A sample from the Hatip Formation, barren of ostracods and foraminifera, contains a displaced assemblage of macroforaminifera (mostly *Nummulites*, *Operculina* and *Discocyclina*) that points to a fan delta environment.

4. GEOCHEMISTRY OF THE VOLCANISM IN THE TAŞCILAR BASIN

Three samples were analyzed to examine the petrogenesis of the syn-sedimentary volcanism in the Taşcilar basin (Appendix S6). The samples are classified as subalkaline basalts and exhibit enrichment in incompatible elements compared to N-MORB (Figure 6b). Negative Nb anomalies are present, which may be due to contamination by continental crust and/or a contribution from metasomatized subcontinental lithospheric mantle (SCLM). However, enrichment levels in the Taşcilar lavas are very low compared with lithologies involving a dominant contribution from SCLM (such as lamproites) (e.g. Gibson et al. 1993). This may suggest a role for asthenospheric melts that have been contaminated by continental lithosphere (via mixing with melts of metasomatized SCLM and/or contamination with continental crust) (Figure 6c). The slightly fractionated HREE patterns may indicate mixing of garnet-facies and spinel-facies melts (Figure 6c). The overall geochemical characteristics suggest that the Tascilar magmatism was triggered by decompression associated with stretching of the continental lithosphere.

5. DISCUSSION AND GEODYNAMIC IMPLICATIONS

The tectono-stratigraphic results indicate that the Taşcilar sedimentary succession was deposited in a basin whose evolution was strongly controlled by strike-slip tectonics, showing typical pull-apart basin features such as basin asymmetry, rapid subsidence and uplift stages, abrupt lateral facies changes and unconformities (Christie-Blick & Biddle, 1985). The different fault-bounded basin sectors characterized by different stratigraphies indicate the syn-sedimentary nature of the faults. Subsidence is highlighted by the deepening of the sedimentary facies, which evolved from continental to shallow marine to relatively deep marine environments (outer neritic–upper bathyal environments; Figure 5). The subsident trend stops at the unconformity between the Taşcilar and Hatip Formations. The unconformity and the palaeo-environment indicate a shallowing of the basin, which is interpreted as an uplift driven by transpressive faulting. The change from tectonic subsidence to uplift was driven by the inversion of the stress regime from transtensive to transpressive. This tectonic inversion fits with the results of the structural analysis, allowing us to propose a two-stage tectonic model for the onset and development of the Taşcilar pull-apart basin. The first tectonic stage, which included the nucleation of the basin, was generated by the activation of releasing step-over areas along sinistral strike-slip master faults (Figure 3d). The contemporary development of synthetic and antithetic high-angle faults set up the transtensional conditions for the formation of the pull-apart basin, where the deposition started in a context of fast subsidence. The second tectonic stage was characterized by a WNW–ESE-directed σ_1 axis transpressional tectonic regime (Figure 3e), with the consequent reactivation of the master faults as dextral strike-slip faults in agreement with the general strike-slip movement of the NASZ.

The results of the nannofossil biostratigraphy constrain the age of the Taşcilar Formation to between the upper part of the CNE4 Zone and the lower part of the CNE5 Zone, indicating the middle part of the early Eocene. The deposition age of the Hatip Formation is constrained to the middle part of the early Eocene CNE5 Zone. The lower, undated, Delibey Formation, which is characterized by a high sedimentation rate and reduced thickness, can be confidently ascribed to the early Eocene.

Overall, our new data indicate that the Taşcilar pull-apart basin developed within a strike-slip tectonic regime during the Ypresian (early Eocene). The first implication of our results is that the strike-slip movements linked to the onset of the NASZ were likely established in the Ypresian, after the Selandian (middle Palaeocene) collision between the Sakarya and Istanbul-Zonguldak terranes. The collision age is constrained by the age of the ophiolite-bearing mass gravity deposits deposited in a foredeep basin immediately before the collision (Taraklı Flysch; Catanzariti et al., 2013). The transcurrence along the Intra-Pontide suture zone after the continental collision could have been triggered by oblique collision, which was suggested as the process for the closure of the Intra-Pontide ocean (Göncüoğlu & Erendil, 1990).

The post-collisional activation of the NASZ along the Intra-Pontide suture zone is consistent with the large-scale strike-slip faulting affecting suture zones that has been recognized as a characteristic of continental collisions (McKenzie, 1972; Molnar and Tapponier, 1975; Tapponier et al., 1982; Dewey et al., 1986; Phillips et al., 2004, and references therein).

The post-collisional evolution of northern Turkey across the Intra-Pontide suture zone can thus be delineated (Figure 7). In the Ypresian, inside the Intra-Pontide suture zone, strike-slip activity of the NASZ started within a transtensional tectonic regime characterized by a NE–SW-directed σ_1 axis (Figure 7a). The post-collisional Eocene volcanism, confined to a narrow band trending parallel to the Intra-Pontide suture zone (Keskin et al., 2008; Altunkaynak and Dilek, 2013), can be related to transcurrence along the NASZ, as is the case for the volcanism associated with the Taşcilar pull-apart basin. The switch from a transtensional to a transpressional regime, related to the rotation of the σ_1 axis from NE–SW to WNW–ESE, occurred during the upper part of the

Ypresian (Figure 7b). After the initiation of strike-slip faulting, displacements along the NASZ have continued up to the Present with successive steps (Zattin et al., 2010 and references therein; Yolsal-Çevikbilen et al., 2012 and references therein) involving a progressively wider deformation zone. During this long evolution, the late Miocene represents a main step of fault activity intensification (Figure 7c; Uysal et al., 2006) rather than the age of NASZ onset (Şengör et al., 2005).

The radiometric data on fault gouges that document the onset of significant strike-slip faulting along the NASZ in the Eocene (ca 57 Ma, Uysal et al., 2006; ca 40 Ma, Boles et al., 2015) can be reconsidered in the proposed geodynamic scenario.

The presented results contribute to the discussion about the geodynamic interactions between the Anatolia, Arabia and Eurasia plates (e.g., Jolivet & Faccenna, 2000; Faccenna et al., 2006; Okay et al., 2010; Jolivet et al., 2013). Our study documents that dextral strike-slip faulting in an E–W direction in the central sector of the NASZ developed in the Ypresian, consequently indicating that the westward translation of the Anatolian plate started during the early Eocene. The inception of the westward translation of the Anatolian plate in the middle Eocene, or even earlier, has also been indicated by the age of dextral mylonitic shearing from the westernmost part of the NASZ (Türkoğlu et al., 2016).

The geochemistry of the syn-sedimentary subalkaline basalts from the Taşcilar basin points to the asthenospheric upper mantle as the main source of the Ypresian magmatism, supporting the idea that the NASZ propagated through the lithosphere (cf. Fichtner et al., 2013) as a long-lived strike-slip deformation zone formed along the Intra-Pontide suture zone.

6. CONCLUSIONS

Our data on the Taşcilar pull-apart basin provide biostratigraphical constraints for the Ypresian onset of the lithospheric strike-slip deformation along the Intra-Pontide suture zone that started the generation of the NASZ. The proposed geodynamic model indicates that the westward escape of the Anatolian plate began in the early Eocene.

ACKNOWLEDGMENTS

The authors are grateful to Tuncay Taymaz, Gernold Zulauf, an anonymous reviewer, the Associate Editor David Westerman and the Scientific Editor Carlo Doglioni. The manuscript has benefited greatly from their constructive reviews. This research was supported by MIUR-PRIN Project 2010-2011 (resp. M. Marroni) and by IGG-CNR.

REFERENCES

Agnini, C., Fornaciari, E., Raffi, I., Catanzariti, R., Palike, H., Backman, J., & Rio, D. (2014). Biozonation and biochronology of Paleogene calcareous nannofossils from low and middle latitudes. *Newsletters on Stratigraphy*, 47, 131-181.

Altunkaynak, Ş., & Dilek, Y. (2013). Eocene mafic volcanism in northern Anatolia: its causes and mantle sources in the absence of active subduction. *International Geological Review*, 55, 1641–1659.

Ambraseys N.N. (1970). Some characteristic features of the North Anatolian Fault Zone. *Tectonophysics*, 9, 143–65.

Armijo, R., Meyer, B., Hubert-Ferrari, A., & Barka, A., (1999). Westward propagation of North Anatolian Fault into the Northern Aegean: timing and kinematics. *Geology*, 27, 267-270.

Barka, A.A. (1992). The North Anatolian fault Zone. *Annales Tectonicae,* 6. 164-195.

Barka, A., Akyüz, H.S., Cohen, H.A., & Watchorn, F. (2000). Tectonic evolution of the Niksar and Tasova-Erbaa pull-apart basins, North Anatolian Fault Zone: their significance for the motion of the Anatolian Block. *Tectonophysics*, 322, 243-264.

Berggren, W.A., & Miller, K.G. (1989). Cenozoic bathyal and abyssal calcareous benthic foraminiferal zonation. *Micropaleontology*, 35, 308-320.

Boles, A., van der Pluijm, B.A., Mulch, A., Mutlu, H., Tonguc, U. & Warr, L.N. (2015). Hydrogen and $^{40}Ar/^{39}Ar$ isotope evidence for multiple and protracted paleofluid flow events within the long-lived North Anatolian Keirogen (Turkey). *Geochemistry, Geophysics, Geosystems,* 16, 1975-1987.

Catanzariti, R., Ellero, A., Göncüoğlu, M.C., Marroni, M., Ottria, G., & Pandolfi L. (2013). The Taraklı Flysch in the Boyalı area (Sakarya Terrane, Northern Turkey): Implications for the tectonic history of the Intrapontide Suture Zone. *Comptes Rendus Geosciences*, 345, 454-461.

Christie-Blick, N. & Biddle, K. T. (1985). Deformation and basin formation along strike-slip faults. In K.T. Biddle, & N. Christie-Blick, (*Eds*.), *Strike-Slip Deformation, Basin Formation, and Sedimentation: SEPM Special Publications*, 37, 1–34.

Dall'Antonia, B., Bossio, A., & Guernet, C. (2003). The Eocene/Oligocene boundary and the psychrospheric event in the Tethys as recorded by deep-sea ostracods from the Massignano Global Boundary Stratotype Section and Point, Central Italy. *Marine Micropaleontology*, 48, 91-106.

Delvaux, D., & Sperner, B. (2003). Stress tensor inversion from fault kinematic in-dicators and focal mechanism data: the TENSOR program. In D. Nieuwland, (*Ed.), New Insights into*

Structural Interpretation and Modelling: Geological Society, London, Special Publications, 212, 75-100.

Dewey, J.F., Hempton, M.R., Kidd,W.S.F., Saroglu, F., Şengör, A.M.C. (1986). Shortening of continental lithosphere: the neotectonics of Eastern Anatolia – a young collision zone. In: Coward, M.P., Ries, A.C. (Eds.), Collosion Tectonics: *Geological Society Special Publications*, 19, 3-36.

Ellero, A., Ottria, G., Marroni, M., Pandolfi, L., & Göncüoğlu, M.C. (2015a). Analysis of the North Anatolian Shear Zone in Central Pontides (northern Turkey): insight for geometries and kinematics of deformation structures in a transpressional zone. J*ournal of Structural Geology*, 71, 124-141.

Ellero, A., Ottria, G., Sayit, K., Catanzariti, R., Frassi, C., Göncüoğlu, M.C., Marroni, M., & Pandolfi, L. (2015b). Geological and geochemical evidence for a Late Cretaceous continental arc in the Central Pontides, Northern Turkey. *Ofioliti*, 40, 73-90.

Faccenna, C., Bellier, O., Martinod, J., Piromallo, C. & Regard, V. (2006). Slab detachment beneath eastern Anatolia: A possible cause for the formation of the North Anatolian fault. *Earth and Planetary Science Letters*, 242, 85-97.

Fichtner, A., Saygin, E., Taymaz, T., Cupillard, P., Capdeville, Y., & Trampert, J. (2013). The deep structure of the North Anatolian Fault Zone. *Earth and Planetary Science Letters*, 373, 109-117.

Frassi, C., Göncüoğlu, M.C., Marroni, M., Pandolfi, L., Ruffini, L., Ellero, A., Ottria, G., & Sayit, K. (2016). The Intra-Pontide suture zone in the Tosya-Kastamonu area, Northern Turkey. *Journal of Maps*, 12, 211-219.

Gibson, S.A., Thompson, R.N., Leat, P.T., Dickin, A.P., Morrison, M.A., Hendry, G.L., Dickin, A.P., & Mitchell, J.G. (1993). Ultrapotassic along the flanks of the Oligo-Miocene Rio Grande Rift, USA: Monitors of the zone of lithospheric mantle extension and thinning beneath a continental rift. *Journal of Petrology*, 34, 187–228.

Göncüoğlu, M.C., & Erendil, M. (1990). Pre-Late Cretaceous tectonic units of the Armutlu Peninsula. Proceedings of the 8th Turkish Petrological Congress, 8, 161-168.

Göncüoğlu M. C., Gürsu S., Tekin U. K. & Koksal S. (2008). New data on the evolution of the Neotethyan oceanic branches in Turkey: Late Jurassic ridge spreading in the Intra-Pontide branch. *Ofioliti*, 33, 153-164.

Göncüoğlu M. C., Maroni, M., Sayit, K., Tekin U. K., Ottria G., Pandolfi, L. & Ellero, A. (2012). The Ayli Dag ophiolite sequence (central-northern Turkey): A fragment of middle Jurassic oceanic lithosphere within the Intra-Pontide suture zone. *Ofioliti*, 37, 77-91.

Göncüoğlu, M.C., Marroni, M., P&olfi, L., Ellero, A., Ottria, G., Catanzariti, R., Tekin, U.K., & Sayit, K. (2014). The Arkot Dağ Mélange in Araç area, central Turkey: Evidence of its origin within the geodynamic evolution of the Intra-Pontide suture zone. *Journal of Asian Earth Sciences*, 85, 117-139.

Hubert-Ferrari, A., Armijo, R., King, G., Meyer, B., & Barka, A. (2002). Morphology, displacement, and slip rates along the North Anatolian Fault, Turkey. *Journal of Geophysics Research*, 107 (B10), 2235.

Hubert Ferrari, A., King, G., van der Woerd, J., Villa, I., Altunel, E., & Armijo, R. (2009). Long-term evolution of the North Anatolian Fault: new constraints from its eastern termination. In D.J.J. van Hinsbergen, M.A Edwards & R. Govers (Eds.*), Collision and Collapse at the Africa-Arabia-Eurasia Subduction Zone. Geological Society, London, Special Publication,* 311, 133-154.

Kaymakçı, N., Stanley, H.W., & Vandijk, P.M. (2003). Kinematic and structural development of the Çankırı Basin (Central Anatolia, Turkey): a paleostress inversion study. *Tectonophysics*, 364, 85-113.

Keskin, M., Genç, SC., & Tüysüz, O. (2008). Petrology and geochemistry of post collisional Middle Eocene volcanic units in North-Central Turkey: evidence for magma generation by slab breakoff following the closure of the Northern Neotethys Ocean. *Lithos*, 104, 267-305.

Kind, R., Eken, T., Tilmann, F., Sodoudi, F., Taymaz, T., Bulut, F., Yuan, X., Can, B., & Schneider, F. (2015). Thickness of the lithosphere beneath Turkey and surroundings from S-receiver functions. *Solid Earth*, 6, 971–984.

Koçyiğit, A., Yılmaz, A., Adamia, S., & Kuloshvili, S. (2001). Neotectonics of East Anatolian Plateau (Turkey) and Lesser Caucasus: implications for transition from thrusting to strike-slip faulting. *Geodinamica Acta*, 14, 177-195.

McKenzie, D. (1972). Active Tectonics of Mediterranean Region. *Geophysical Journal International*, 30, 109-185.

Molnar, P., & Tapponnier, P. (1975). Cenozoic Tectonics of Asia: Effects of a Continental Collision. *Science*, 189, 419-426.

Nemec, W. & Steel, R.J. (1984). Alluvial and coastal conglomerates: Their significant features and some comments on gravelly mass-flow deposits. In E.H. Koster & R.J. Steel (Eds.), *Sedimentology of Gravels and Conglomerates. Canadian Society of Petroleum Geologist*, 10, 1–31.

Okay, A.I., & Tüysüz, O. (1999). Tethyan sutures of northern Turkey. In B. Durand, L. Jolivet, F. Horvath & M. Seranne (Eds.), *The Mediterranean Basins: Tertiary*

Extension within the Alpine Orogen. Geological Society, London, Special Publication 156, 475–515.

Okay, A.I., Tüysüz, O., Satır, M., Özkan-Altıner, S., Altıner, D., Sherlock, S., & Eren, R.H., (2006). Cretaceous and Triassic subduction-accretion, HP/LT metamorphism and continental growth in the Central Pontides, Turkey. *Geological Society America Bulletin*, 118, 1247-1269.

Okay, A. I., Sunal, G., Sherlock, S., Altıner, D., Tüysüz, O., Kylander-Clark, A. R. C. & Aygül M. (2013). Early Cretaceous sedimentation and orogeny on the active margin of Eurasia: Southern Central Pontides, Turkey. *Tectonics*, 32, 1247-1271.

Okosun, E. A. & Osterloff, P. (2014). Ostracod, Diatom and Radiolarian Biostratigraphy of the Niger Delta, Nigeria. *Earth Science Research*, 3, 72-93.

Pearce, J. A., (1996). A users guide to basalt discrimination diagrams. In D. A. Wyman (Ed.), *Trace Element geochemistry of volcanic rocks: Applications for massive sulphide exploration. Geological Association of Canada, Short Course Notes*, 12, 79-113.

Phillips, R.J., Parrish, R.R., & Searle M.P. (2004). Age constraints on ductile deformation and long-term slip rates along the Karakoram fault zone, Ladakh. Earth and Planetary Science Letters, 226, .305-319.

Sayit, K., Marroni, M., Göncüoğlu, M.C., P&olfi, L., Ellero, A., Ottria, G., & Frassi, C. (2016). Geological setting and geochemical signatures of the mafic rocks from the Intra‑Pontide Suture Zone: implications for the geodynamic reconstruction of the Mesozoic Neotethys. *International Journal of Earth Sciences*, 105, 39-64.

Şengör, A.M.C., Tüysüz, O., Imren, C., Sakinc, M., Eyidogan, H., Görür, N., Le Pichon, X., & Rangin, C. (2005). The North Anatolian Fault: A New Look. *Annual Review of Earth and Planetary Sciences*, 33, 37-112.

Şengör, A.M.C., & Yılmaz, Y. (1981). Tethyan evolution of Turkey: a plate tectonic approach. *Tectonophysics*, 75, 181-241.

Sohn, Y.K., Kim, S.B., Hwang, I.G., Bahk, J.J., Choe, M.Y. & Chough, S.K. (1997). Characteristics and depositional processes of large-scale gravely gilbert-type foresets in the Miocene Doumsan fan delta, Pohang Basin, SE Korea. *Journal of Sedimentary Research*, 67, 130–141.

Sohn, Y.K. & Son, M. (2004). Synrift stratigraphic geometry in a transfer zone coarse-grained delta complex, Miocene Pohang Basin, SE Korea. *Sedimentology*, 51, 1387-1408.

Sun, S.S., & McDonough, W.F. (1989). Chemical and isotopic systematics of oceanic basalts: implications for mantle composition and processes. In A.D. Saunders & M.J. Norry (Eds.), *Magmatism in the Ocean Basins: Geological Society of London, Special Publication*, 42, 313-345.

Sunal, G., & Tüysüz, O. (2002). Palaeostress analysis of Tertiary post-collisional structures in the Western Pontides, northern Turkey. *Geological Magazine*, 139, 343-359.

Tapponnier, P., Peltzer, G., Le Dain, A.Y., Armijo R., & Cobbold, P. (1982). Propagating extrusion tectonics in Asia: New insights from simple experiments with plasticine. *Geology*, 10, 611-616.

Tatar, O., Yurtmen, S., Temiz, H., Gürsoy, H., Koçbulut, F., Mesci, B.L., & Guezou, J.C. (2007). Intracontinental Quaternary volcanism in the Niksar pull-apart basin, North Anatolian Fault Zone, Turkey. *Turkish Journal of Earth Sciences*, 16, 417-440.

Türkoğlu, E., Zulauf, G., Linckens, J., & Ustaömer, T. (2016). Dextral strike‐slip along the Kapıdağ shear zone (NW Turkey): evidence for Eocene westward translation of the Anatolian plate. *International Journal of Earth Sciences*, 105, 2061-2073.

Uysal, I.T., Mutlu, H., Altunel, E., Karabacak, V., & Golding, S.D. (2006). Clay mineralogical and isotopic (Ke-Ar, $\delta^{18}O$, δD) constraints on the evolution of the North Anatolian Fault Zone, Turkey. *Earth and Planetary Science Letters*, 243, 181-194.

Winchester, J. A., & Floyd, P. A. (1977). Geochemical discrimination of different magma series and their differentiation products using immobile elements. *Chemical Geology*, 20, 25-343.

Yolsal-Çevikbilen, S., Biryol, C.B., Beck, S., Zandt, G., Taymaz, T., Adıyaman, H.E., & Özacar, A.A. (2012). 3-D crustal structure along the North Anatolian Fault Zone in north-central Anatolia revealed by local earthquake tomography. *Geophysical Journal International*, 188, 819-849.

Zattin, M., Okay, A.I., & Cavazza, W. (2005). Fission-track evidence for late Oligocene and mid-Miocene activity along the North Anatolian Fault in southwestern Thrace. *Terra Nova*, 17, 95-101.

Zattin, M., Cavazza, W., Okay, A.I., Federici, I., Fellin, M.G., Pignalosa, A., & Reiners, P. (2010). A precursor of the North Anatolian Fault in the Marmara Sea region. *Journal of Asian Earth Sciences*, 39, 97-108.

FIGURE CAPTIONS

Figure 1. Tectonic map of the eastern Mediterranean–Middle East region (modified from Barka, 1992 and Ellero et al., 2015a). ISZ: Intra-Pontide suture zone. Yellow arrows show current relative plate motion with respect to Eurasia. Solid lines are strike-slip faults; lines with triangles are thrust faults. The offshore tectonic lineaments are indicated in white.

Figure 2. (a) Simplified geological map of the Central Pontides (Northern Turkey), showing the location of the study area. (b) Geological sketch map and geological cross-section of the Taşcilar basin. The rose diagrams, displaying the strike and dip of the main mapped faults (27 data), highlight the occurrence of two main systems of high-angle faults trending NNE–SSW and roughly E–W.

Figure 3. Statistical analysis of all the faults measured in the Taşcilar basin (107 data) highlighted that faults are predominantly high-angle (>60°) strike-slip faults trending along three main directions: about E–W, NE–SW and about N–S. (a) Orientation statistics of poles to fault planes. (b,c) Diagrams showing the dips of the fault planes and the plunges of slickensides on the faults, respectively. (d,e) Palaeostress strike-slip tensors from five measurement stations of mesoscale brittle structures (see locations in Appendix S1). Stereograms show traces of strike-slip faults with observed slip lines and slip senses (equal-area stereographic projections, lower hemisphere). The principal stress axes (σ_1, σ_2, σ_3) and types of stress tensor were obtained using the Win_TENSOR software (Delvaux & Sperner, 2003).

Figure 4. Field occurrence of the main lithologies recognized in the Taşcilar basin. (a,b) The Delibey Formation consists of an about 180 m thick succession of polymict poorly sorted and clast-supported crudely stratified rudites and arenitic-rudites. In (b) the Delibey Formation close to the fault-bounded northern margin of the Taşcilar basin shows an almost vertical bedding surface (S0). (c) Coarse-grained matrix-supported rudites of the Taşcilar Formation. (d) Marine ruditic-arenites of the Taşcilar Formation. Cross-bedding, clay chips and an erosive surface are indicated. (e) Fine-grained arenites and pelites (thin-bedded facies) in the upper part of the Taşcilar Formation, showing the lenticular shape (arrows) of the arenitic interval. (f) Angular unconformity between the Hatip Formation and the Taşcilar Formation. The Hatip Formation is characterized by thick and coarse-grained clast-supported conglomerates interbedded with minor coarse- to fine-arenites and rare marls. The bedding surface (S0) in the Taşcilar Formation is indicated.

Figure 5. Representative stratigraphy and biostratigraphy of the Taşcilar basin succession. Palaeobathymetry and depositional environments scheme modified from Okosun & Osterloff (2014); bathymetric range for the upper bathyal interval from Berggren & Miller (1989); the dark blue intervals are those constrained by micropalaeontological data. IPSZ: Intra-Pontide suture zone. A detailed stratigraphic log of the sampled interval and the complete micropalaeontological database are provided in Appendices S2, S3 and S4, respectively.

Figure 6. (a) Field occurrence of basalts in the Taşcilar basin. The emplacement of the volcanic rocks produced syn-sedimentary deformation in poorly lithified sediments (pelites of the Taşcilar Formation). Arrows indicate the “soft sediment” deformation. (b) Chemical classification of the

Taşcilar basalts (after Winchester and Floyd 1977, modified by Pearce 1996). (c) Trace element and REE patterns of the Taşcilar basalts (normalization values from Sun and McDonough 1989). The samples display some gains and losses in elements with low ionic potential (e.g. Ba, Rb and Sr), which can be attributed to the alteration. The high field strength elements and REE, however, appear to have remained immobile, thus reflecting the pristine chemistry.

Figure 7. Block diagrams illustrating the post-collisional geodynamic evolution of northern Anatolia across the Intra-Pontide suture zone, from (a,b) the Ypresian (early Eocene) to (c) the late Miocene. IZT: Istanbul-Zonguldak Terrane; ISZ: Intra-Pontide suture zone; SAT: Sakarya Terrane; NASZ: North Anatolian Shear Zone. For constraints on the current lithosphere–asthenosphere boundary depth and tomographic models of northern Anatolia see Fichtner et al. (2013) and Kind et al. (2015).

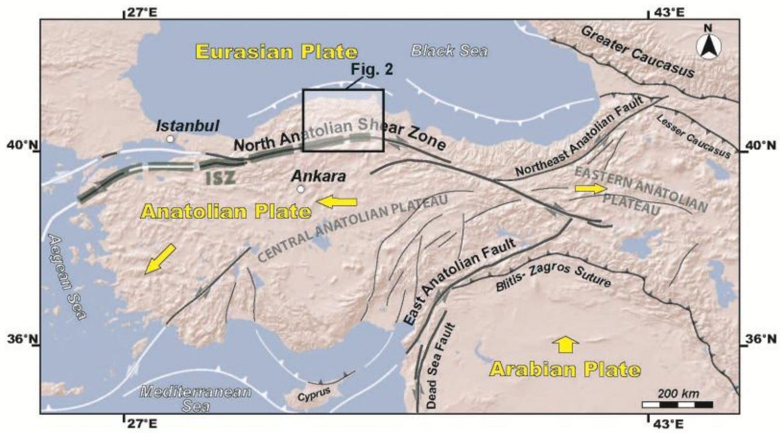
27°E
43°E
40°N
36°N
N
Eurasian Plate
Black Sea
Fig. 2
Greater Caucasus
Lesser Caucasus
Istanbul
North Anatolian Shear Zone
Northeast Anatolian Fault
ISZ
Ankara
Anatolian Plate
CENTRAL ANATOLIAN PLATEAU
EASTERN ANATOLIAN PLATEAU
Aegean Sea
East Anatolian Fault
Bitlis- Zagros Suture
Dead Sea Fault
Arabian Plate
Mediterranean Sea
Cyprus
200 km

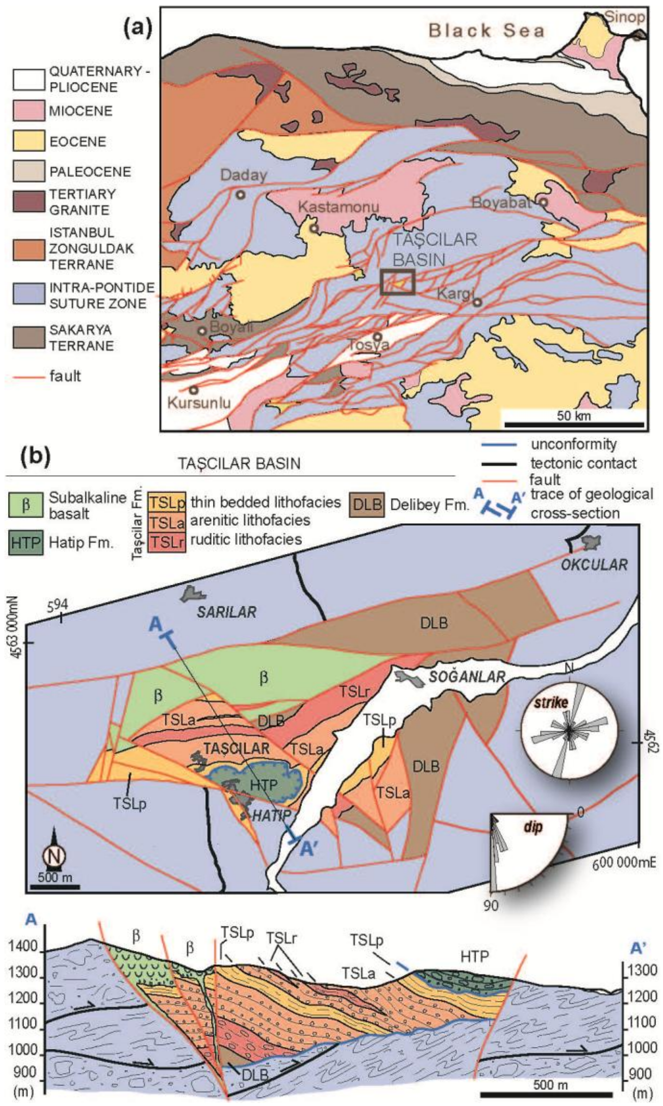
(a)
Black Sea
Sinop
QUATERNARY - PLIOCENE
MIOCENE
EOCENE
PALEOCENE
TERTIARY GRANITE
ISTANBUL ZONGULDAK TERRANE
INTRA-PONTIDE SUTURE ZONE
SAKARYA TERRANE
fault
Daday
Kastamonu
Boyabat
TAŞCILAR BASIN
Kargi
Boyali
Tosya
Kursunlu
50 km
(b)
TAŞCILAR BASIN
unconformity
tectonic contact
fault
trace of geological cross-section
β Subalkaline basalt
HTP Hatip Fm.
Taşcilar Fm.
TSLp thin bedded lithofacies
TSLa arenitic lithofacies
TSLr ruditic lithofacies
DLB Delibey Fm.
OKCULAR
SARILAR
594
4563 000mN
DLB
SOĞANLAR
TSLr
TSLa
TSLp
TAŞCILAR
HTP
HATIP
strike
dip
0
90
600 000mE
500 m
A
A'
1400
1300
1200
1100
1000
900
(m)
HTP
500 m

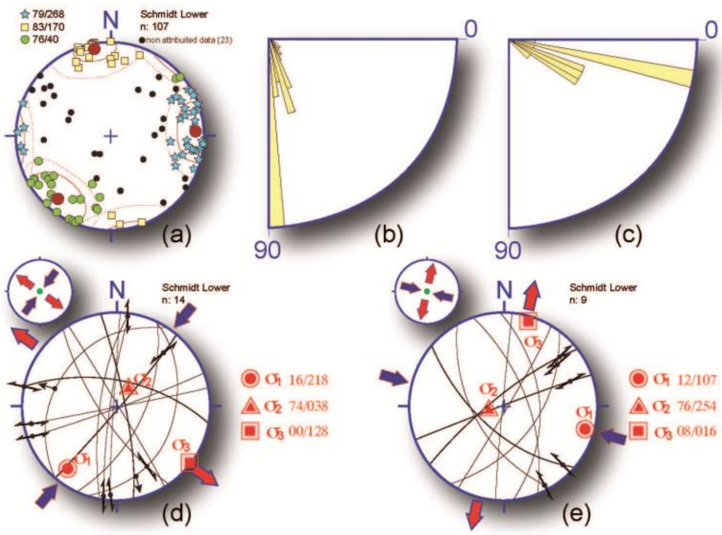

79/268
83/170
76/40
N
Schmidt Lower
n: 107
non attributed data (23)
(a)
0
90
(b)
0
90
(c)
N
Schmidt Lower
n: 14
σ1 16/218
σ2 74/038
σ3 00/128
(d)
N
Schmidt Lower
n: 9
σ1 12/107
σ2 76/254
σ3 08/016
(e)

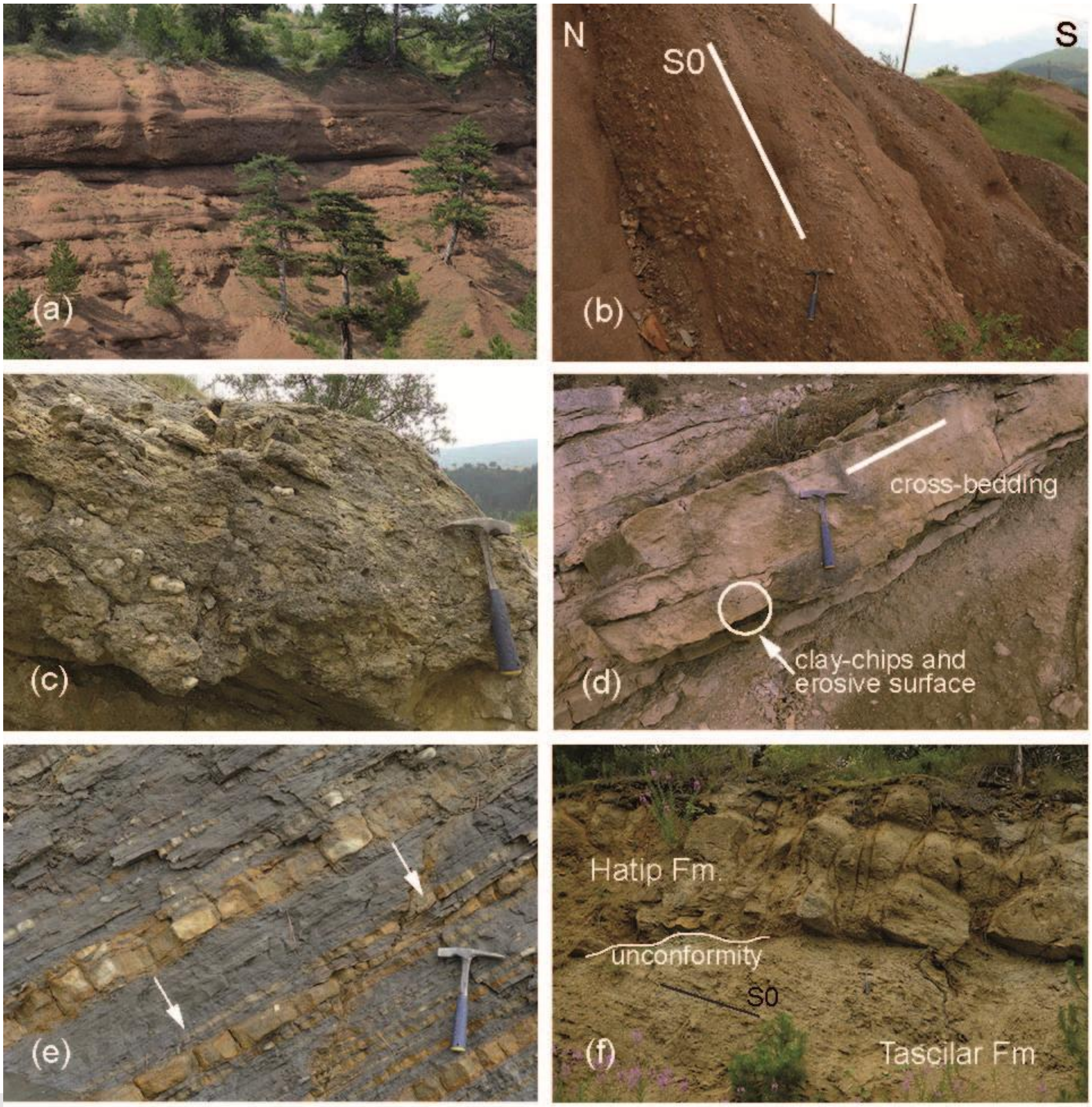
(a)
N
S
S0
(b)
(c)
cross-bedding
clay-chips and
erosive surface
(d)
(e)
Hatip Fm.
unconformity
S0
Tascilar Fm
(f)

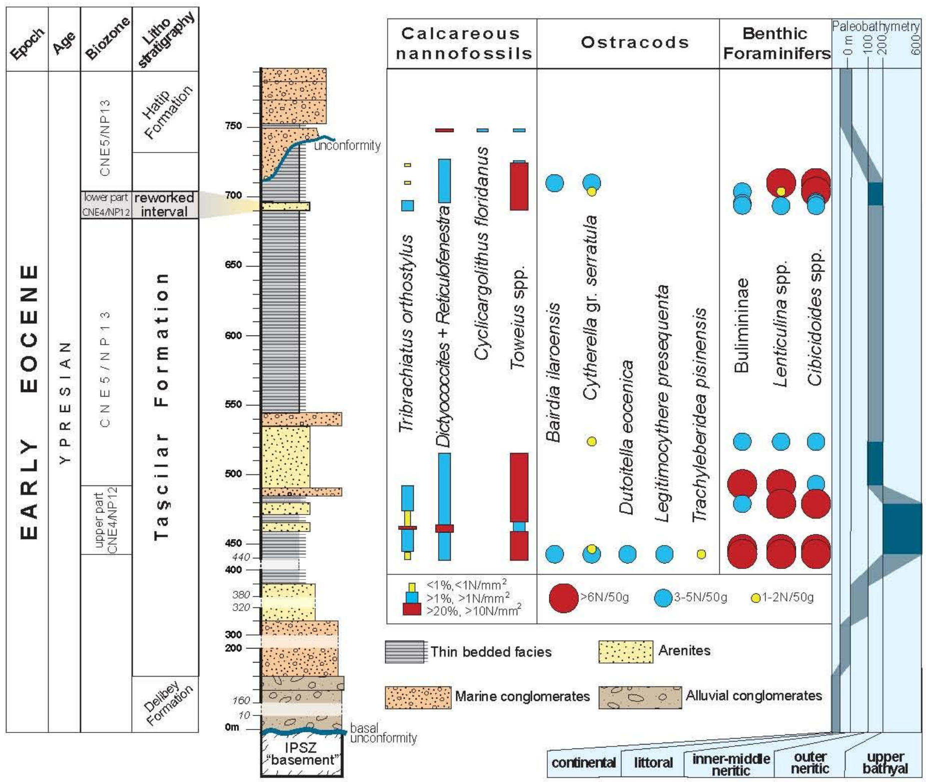
Epoch
Age
Biozone
Litho stratigraphy
EARLY EOCENE
YPRESIAN
CNE5/NP13
lower part CNE4/NP12
upper part CNE4/NP12
Hatip Formation
reworked interval
Taşcilar Formation
Delibey Formation
unconformity
basal unconformity
IPSZ "basement"
Calcareous nannofossils
Ostracods
Benthic Foraminifers
Paleobathymetry
Tribrachiatus orthostylus
Dictyococcites + Reticulofenestra
Cyclicargolithus floridanus
Toweius spp.
Bairdia ilaroensis
Cytherella gr. serratula
Dutoitella eocenica
Legitimocythere presequenta
Trachyleberidea pisinensis
Buliminiae
Lenticulina spp.
Cibicidoides spp.
<1%,<1N/mm2
>1%, >1N/mm2
>20%, >10N/mm2
>6N/50g
3-5N/50g
1-2N/50g
Thin bedded facies
Arenites
Marine conglomerates
Alluvial conglomerates
continental
littoral
inner-middle neritic
outer neritic
upper bathyal

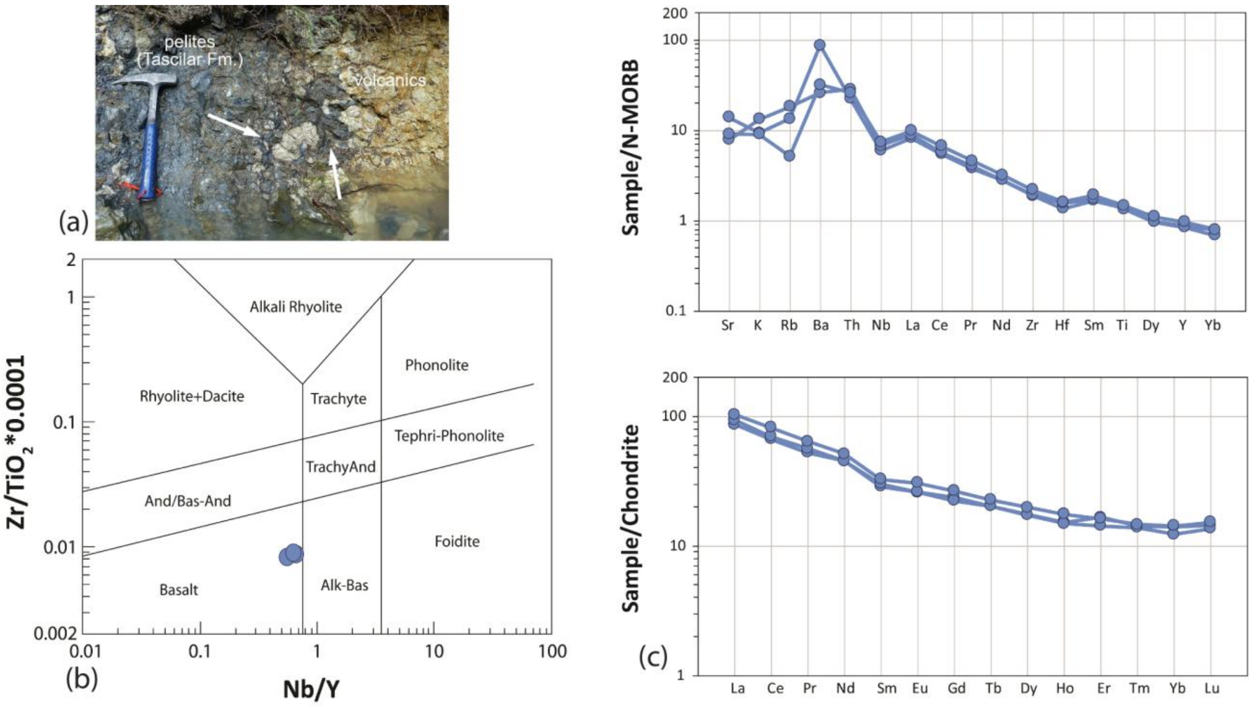

pelites
(Tascilar Fm.)
volcanics
(a)
Alkali Rhyolite
Phonolite
Rhyolite+Dacite
Trachyte
Tephri-Phonolite
TrachyAnd
And/Bas-And
Foidite
Basalt
Alk-Bas
Zr/TiO2 *0.0001
Nb/Y
(b)
Sample/N-MORB
Sr K Rb Ba Th Nb La Ce Pr Nd Zr Hf Sm Ti Dy Y Yb
Sample/Chondrite
La Ce Pr Nd Sm Eu Gd Tb Dy Ho Er Tm Yb Lu
(c)

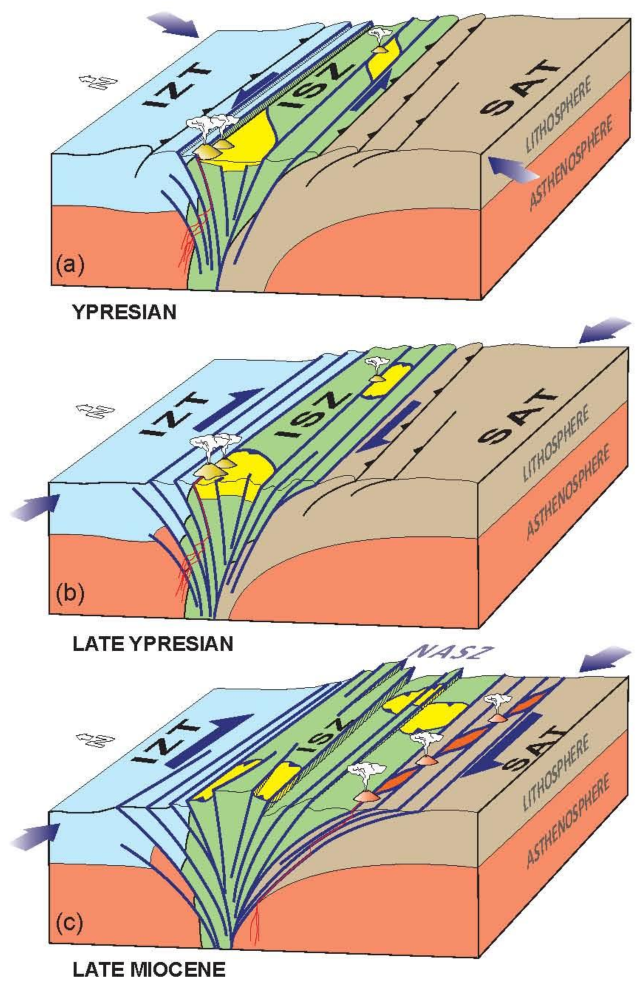
IZT
ISZ
SAT
LITHOSPHERE
ASTHENOSPHERE
(a)
YPRESIAN
(b)
LATE YPRESIAN
NASZ
(c)
LATE MIOCENE